

PROTON STRUCTURE *

Jörg Gayler

for the H1 and ZEUS Collaborations

DESY

Recent inclusive neutral current and charged current DIS data from HERA are discussed in context of pQCD and parton density functions.

1 Introduction

Since the early days of Quantum-Chromo-Dynamics (QCD), deep inelastic scattering (DIS) played a decisive role in stimulating theoretical ideas and testing them experimentally. Now the theory is well established and perturbative QCD (pQCD) is well tested in many processes, but the details of lepton nucleon interactions, in particular at small Bjorken x , and the structure of the proton in terms of parton densities (pdfs) are still objects of intensive research, both, experimentally and theoretically. The understanding of proton structure is of fundamental interest, but also of great practical importance for the quantitative analysis of present and future hadron hadron scattering experiments like those at the forthcoming LHC.

Since its beginning in 1992, the HERA accelerator has been a major source of information on proton structure. The fully inclusive neutral current (NC) and charged current (CC) reactions ($ep \rightarrow eX$ and $ep \rightarrow \nu X$, respectively) are particularly suited to unveil the parton densities of the proton due to the comparatively simple and well understood theoretical description of these reactions.

However, to obtain pdfs at large x and for the decomposition of u and d quark flavours, HERA data are usually combined with results of other experiments, which leads to additional systematic uncertainties. In particular it is desirable to determine the d quark density by the HERA experiments alone, free of nuclear corrections.

This paper deals with collinear pdfs, which contain no information on parton transverse momenta and parton-parton correlations. Constraints on general parton densities

*presented at HSQCD2005, 20 - 24th September, St. Petersburg.

(GPDs) are deduced from some exclusive final states (see [1]), while the constraints on collinear pdfs are obtained from inclusive scattering. After some description of the kinematics and relations of cross sections and structure functions (section 2), I first present shortly the most recent data in CC interactions collected by HERA II, the upgraded HERA machine which provides longitudinally polarised electron and positron beams at the H1 and ZEUS experiments (section 3). Sections 4 and 5 present recent NC and CC data which partially have been used already, for pdf fits, which are described in section 6. The measured contributions of charm and beauty production to the proton structure function is shortly discussed in section 7, followed by conclusions.

2 Cross Sections and Structure Functions

In inclusive ep scattering the proton structure can be probed by γ or Z^0 exchange, i.e. by neutral current interactions, or by W exchange, i.e. by charged current interactions. The NC differential cross section can be expressed in terms of three structure functions, \tilde{F}_2 , \tilde{F}_3 and \tilde{F}_L :

$$d^2\sigma_{NC}^{\pm}/dx dQ^2 = \frac{2\pi\alpha^2}{xQ^4} [Y_+ \cdot \tilde{F}_2 \mp Y_- \cdot x\tilde{F}_3 - y^2 \cdot \tilde{F}_L] \equiv \frac{2\pi\alpha^2}{xQ^4} Y_+ \tilde{\sigma}_{NC}^{\pm}, \quad (1)$$

where $Y_{\pm} = 1 \pm (1-y)^2$. Here, $Q^2 = -q^2$, with q being the four-momentum of the exchanged gauge boson, $x = Q^2/2(P \cdot q)$, the momentum fraction of the proton carried by the parton participating in the interaction, and $y = (P \cdot q)/(P \cdot k)$, the inelasticity, where $k(P)$ is the four-momentum of the incident electron (proton). The term $\tilde{\sigma}_{NC}^{\pm}$ is called “reduced cross section”. It is a combination of structure functions directly related to the differential cross section. The structure function \tilde{F}_2 is the dominant contribution in most of the phase space and can, in leading order (LO) QCD, be written in terms of the quark densities $\sim x \sum_q e_q^2 (q(x) + \bar{q}(x))$. The term $x\tilde{F}_3$, which would vanish in the absence of Z^0 exchange, contributes significantly only at high Q^2 , and is to LO $\sim x \sum_q (q(x) - \bar{q}(x))$, that is, it is given by the valence quarks. The longitudinal contribution \tilde{F}_L is important in Eq. (1) at large y . At small x , to order α_s , $\tilde{F}_L \sim \alpha_s g$, where g is the gluon density.

Similarly, the CC cross section can be written

$$d^2\sigma_{CC}^{\pm}/dx dQ^2 = \frac{G_F^2}{2\pi x} \left(\frac{M_W^2}{Q^2 + M_W^2} \right)^2 \cdot \tilde{\sigma}_{CC}^{\pm}, \quad (2)$$

where G_F is the Fermi coupling constant.

$$\begin{aligned} \text{In LO} \quad \tilde{\sigma}_{CC}^+ &= x[(\bar{u}(x) + \bar{c}(x)) + (1-y)^2(d(x) + s(x))] \\ \text{and} \quad \tilde{\sigma}_{CC}^- &= x[(u(x) + c(x)) + (1-y)^2(\bar{d}(x) + \bar{s}(x))]. \end{aligned}$$

The d -quark density is therefore directly accessible in $e^+p \rightarrow \bar{\nu}_e X$ scattering, avoiding the nuclear corrections necessary when electron deuteron scattering is used.

3 Most Recent HERA Results in inclusive DIS

HERA covers a large phase space in x and Q^2 well suited for pdf analyses, but also for the analysis of electro-weak effects in DIS. Fig. 1 (left) shows NC and CC cross sections spanning three orders of magnitude in Q^2 , which get similar magnitude at $Q^2 \sim 10^4$ where the propagator mass is in the range of M_W^2 . The data thus illustrate electro-weak unification. The standard model (SM) is further tested by the dependence of the CC cross section on the polarisation of the primary electron or positron. The extrapolated cross sections for fully left handed positrons are consistent with zero, the SM expectation (Fig. 1, right). Thus, there is no indication of right handed weak currents (see [2] for further details). For a recent combined electro-weak and pQCD analysis, see [3].

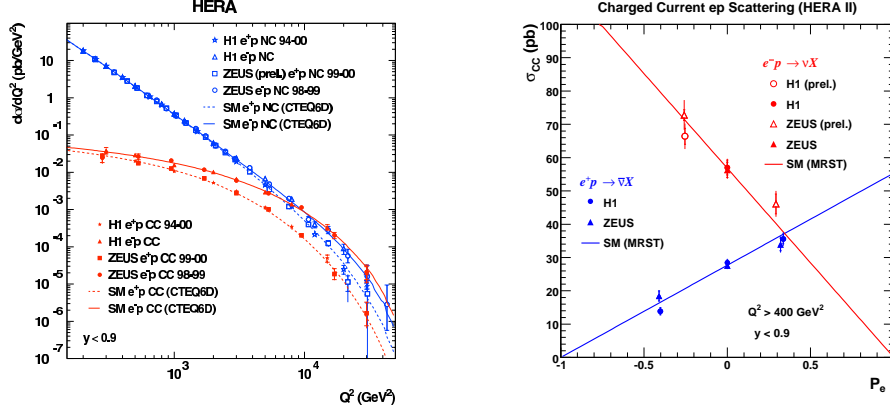


Figure 1: NC and CC cross sections vs. Q^2 (left). Polarisation dependence of the total CC cross section (right).

4 NC data

The HERA I inclusive NC F_2 data are shown in Fig. 2. They span 4 orders of magnitude in x and Q^2 and are closing the gap to the fixed target data. At small x ($x < 0.01$), the

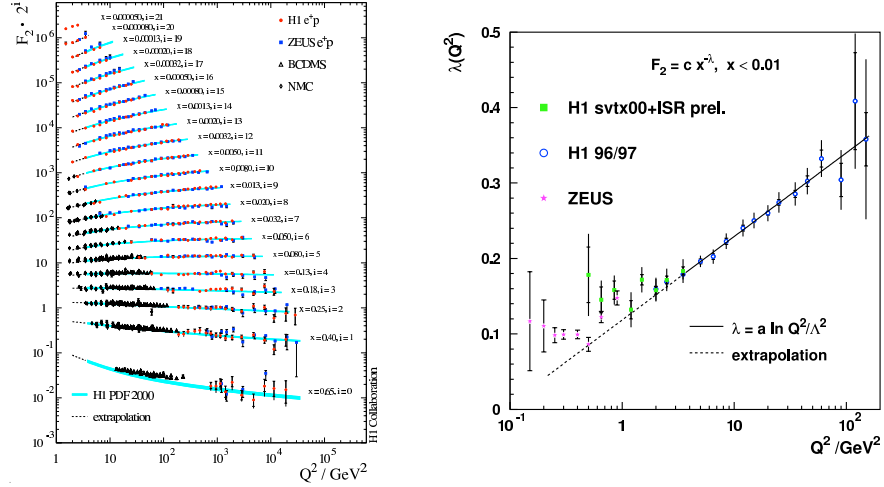


Figure 2: F_2 vs. Q^2 (left). $\lambda(Q^2)$ from fits $F_2 = c(Q^2) \cdot x^{-\lambda(Q^2)}$ for $x < 0.01$ (right).

rise of the structure function towards small x can well be described by $F_2 = c(Q^2) \cdot x^{-\lambda}$ with λ logarithmically rising with Q^2 (Fig. 2, right) and $c(Q^2)$ being roughly constant for $Q^2 > 3$ GeV². At small Q^2 , λ deviates from this logarithmic dependence, consistent with $\lambda \rightarrow 0.08$ for $Q^2 \rightarrow 0$, as expected from soft hadronic interactions.

The longitudinal proton structure function F_L is of considerable interest due to the relation with the proton gluon density, $F_L \sim \alpha_s(Q^2)g(x, Q^2)$. However no direct measurements of F_L are available in the HERA regime. Such measurements require changes of the center of mass energy \sqrt{s} , i.e. of the beam energies. However at very high y , the signature of F_L is a drop of the reduced cross section, because the longitudinal contribution vanishes at $y = 1$. This is visible in Fig. 3, left, for an x distribution at $Q^2 = 4.2$ GeV² [4]¹. The H1 collaboration used various methods with assumptions in the framework of pQCD to exploit this effect. The results are presented in Fig. 3, right, where the

¹It is therefore important to include in pQCD analyses the available reduced cross sections at high y and not F_2 results only.

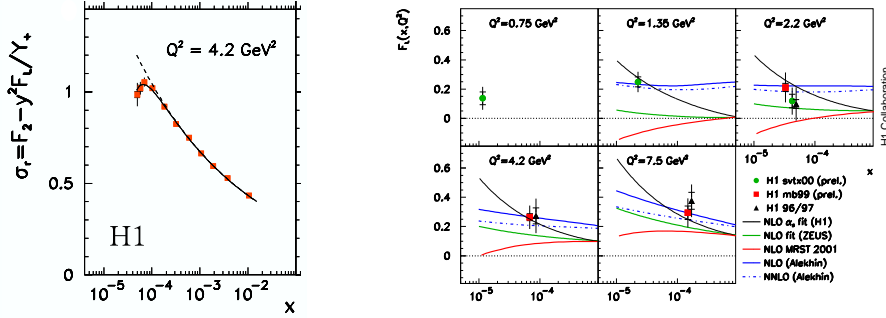


Figure 3: Left: Reduced cross section vs. x for $Q^2 = 4.2 \text{ GeV}^2$. Solid line: fit $\sigma_r = c \cdot x^{-\lambda} - y^2/Y_+ F_L$, broken line: $c \cdot x^{-\lambda}$. Right: $F_L(x, Q^2)$ for fixed Q^2 [4] and theoretical predictions based on [5–8]

determined F_L values are compared with predictions based on the NLO fits of H1 [5], ZEUS [6] and MRST21 [7] and the NLO and NNLO analyses of S. Alekhin [8]. The spread of the predictions is large and shows the importance of direct F_L measurements.

At high x the uncertainties are still quite large (see Fig. 2, left, $x = 0.65$). This led the ZEUS collaboration [9] to apply a new technique, which exploits the fact, that at very high x , where Q^2 can still be well measured using the scattered electron, the hadronic jet vanishes in the beam pipe at small forward angles due to kinematics. If this happens, x is above some x_{edge} depending on Q^2 . Fig. 4 shows x distributions in bins of Q^2 from $Q^2 = 576 \text{ GeV}^2$ to $Q^2 = 5253 \text{ GeV}^2$. In each case, the highest x bin is an average over the x range where the jet vanishes in the beam pipe. These data can provide significant constraints at high x in pQCD analyses.

5 CC data

HERA has the unique possibility to determine the d -quark density in the proton free of nuclear effects by the CC reaction $e^+p \rightarrow \bar{\nu}X$. Fig. 5 shows x distributions at different Q^2 from $Q^2 = 280$ to $Q^2 = 17000 \text{ GeV}^2$. They are dominated by the d -quark for $x > 0.2$ and will, with final HERA statistics, significantly improve the knowledge on the d -quark density. Another constraint is provided by e^+ and e^- NC data at high Q^2 , because u and d quarks enter in $xF_3 \sim 2u_v + d_v$ with weights which differ from those in F_2 .

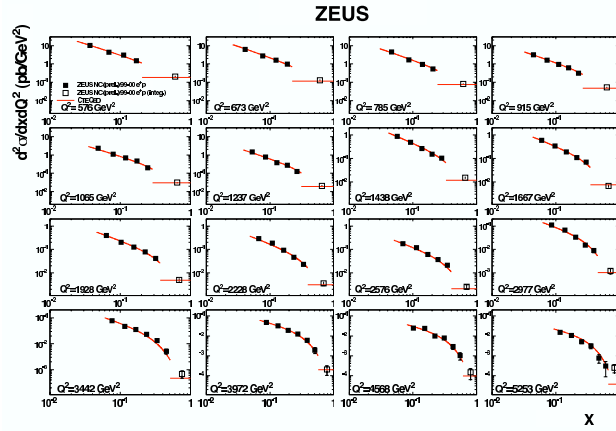


Figure 4: $d\sigma/dx dQ^2$ for NC e^+p compared to SM expectation (CTEQ6D pdfs, solid line).

6 Pdf Fits

Essentially the available information on pdfs at small x is provided by inclusive DIS measurements at HERA, showing in particular a strong rise of the sea and gluon pdfs towards small x . In the standard DIS QCD analyses, a parameterisation of the pdfs at a starting scale Q_0^2 is assumed, which are evolved to higher Q^2 using the NLO DGLAP equations [10]. The parameters at Q_0^2 are then determined by a fit of the calculated cross sections to the data.

The gluon density of the proton at small x is quite well determined, although it influences the cross sections only at next to leading order (NLO) via scaling violations. Di-jet measurements, however, are sensitive to the gluon density already in leading order by boson-gluon fusion (Fig. 6, left). Further, the production of jets at large p_t , with respect to the exchanged boson direction, implies that large momentum fractions of the proton are involved. The correlation of the gluon density with α_s in boson-gluon-fusion is broken by the contributing QCD-Compton graphs (Fig. 6, central and right).

This led the ZEUS collaboration to perform a pdf analysis based on one experiment only by fitting the ZEUS inclusive DIS NC and CC data together with di-jet data measured in photoproduction and inclusive jets in the Breit frame measured in ep DIS [11] (ZEUS-JETS fit). The resulting pdfs, presented in Fig. 7, left, show indeed a reduction of the uncertainty of the gluon density at medium and high x (Fig. 7, right).

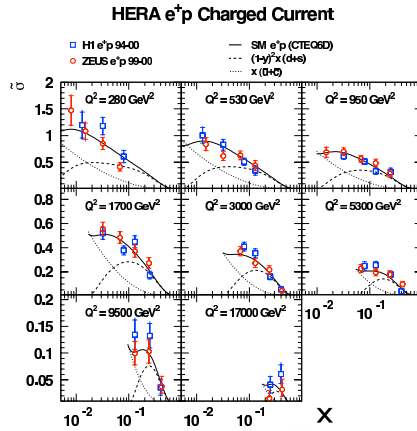


Figure 5: Reduced CC cross sections of H1 and ZEUS as function of x and Q^2 compared with predictions based on CTEQ6D (solid line), showing separately the contributions of $d + s$ (dashed) and $\bar{u} + \bar{c}$ (dotted).

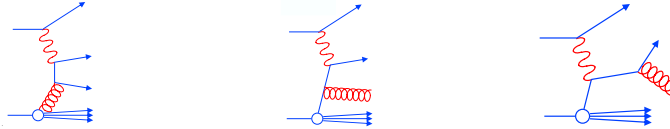


Figure 6: Diagrams for di-jet production. Boson gluon fusion (left), QCD-Compton graphs (central and right).

Other approaches have been used in earlier H1 and ZEUS analyses of inclusive DIS data which differ mainly in the choice of input data used, the handling of systematic errors, the parameterisations at Q_0^2 , and the treatment of heavy quarks.

A special case is the H1 NC analysis [5], based mainly on H1 ep NC data and some BCDMS μp high x data. Here the primary purpose was a determination of the gluon density $g(x)$ and of the strong coupling constant α_s . For this reason, besides $g(x)$ only two functions were parametrised at Q_0^2 , one for the valence and one for the sea quark contribution, with small corrections.

The H1 2000 pdf fit [12], which includes in addition the H1 CC and the BCDMS μd data,² determines $g(x)$ and also the four up and down combinations $U = u + c$, $\bar{U} =$

²The fit was also performed with H1 data alone

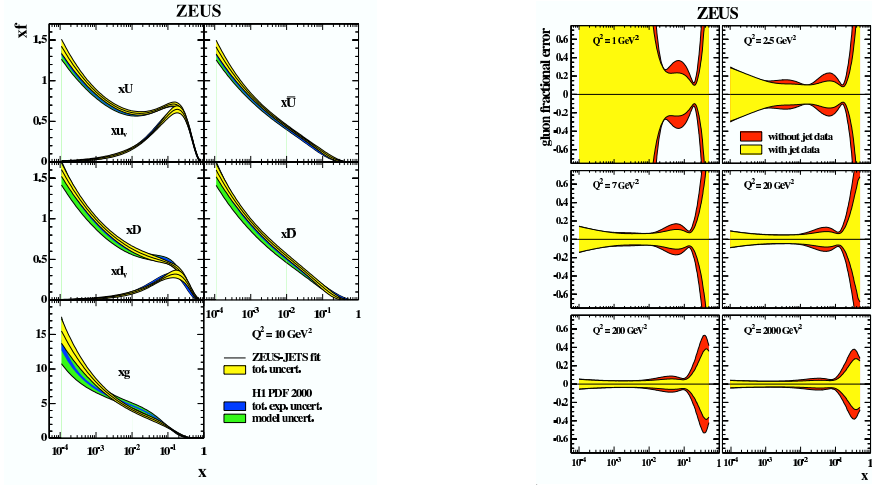


Figure 7: Left: comparison of pdfs from ZEUS-JET and H1 PDF 2000 analyses. Right: experimental uncertainties of the gluon pdf of the ZEUS-JET fit (central error bands) compared to the uncertainties obtained without including the jet data (outer error band).

$\bar{u} + \bar{c}$, $D = d + s$, and $\bar{D} = \bar{d} + \bar{s}$ from which the valence densities $u_v = U - \bar{U}$ and $d_v = D - \bar{D}$ are derived. This fit is compared with the ZEUS-JETS fit in Fig. 7, left. The results are consistent, but differences are visible in the gluon distribution.

The previous ZEUS analysis [6] (“ZEUS-S”) uses ZEUS NC data, μp and μd data from BCDMS, NMC and E665, and CCFR νFe data. Results on $g(x)$, $u_v(x)$, $d_v(x)$, the total sea and $\bar{d} - \bar{u}$ are given.

In Fig 8, the densities of valence quarks, the sea and the gluon are compared for the fits ZEUS-JET, ZEUS-S, H1 PDF 2000 and the global analyses MRST2001 [7] and CTEQ6.1M [13]. In general there is consistency, but one notices that the ZEUS-JET gives lower $g(x)$ at $x \approx 0.01$ and higher valence u and d densities than the other fits.

7 Charm and Beauty Contribution to Proton Structure Functions

There are different schemes to treat the heavy quark contributions and thresholds in pQCD pdf fits. The H1 NC analysis [5] uses the “massive” scheme, which is particularly useful at low Q^2 . In this case the boson gluon fusion contribution (Fig. 6, left) is generated at LO. In the “massless scheme”, favoured for high Q^2 and far above the heavy quark

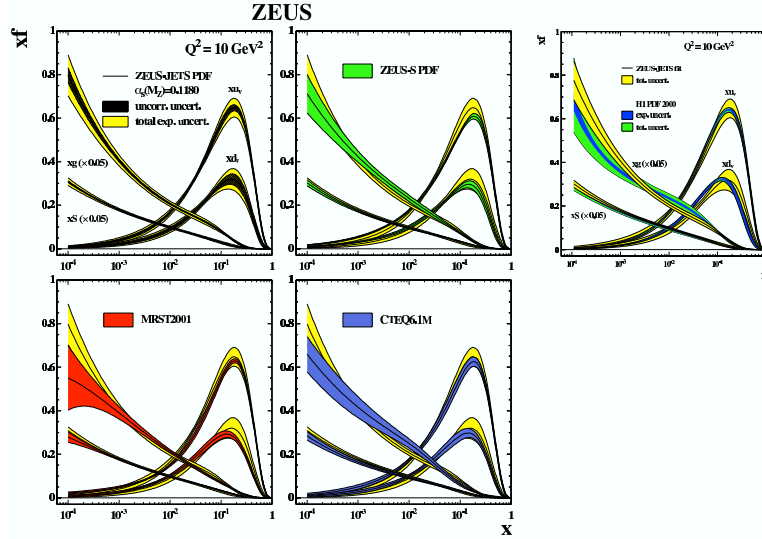


Figure 8: Valence quark, sea and gluon distributions of different NLO analyses. Top row from left to right: ZEUS-JETS, ZEUS-S and ZEUS-JETS together with H1 PDF 2000. Bottom row: ZEUS-JETS with MRST 2001 [7] (left) and CTEQ6.1M [13] (right).

production thresholds, the heavy quarks appear as part of the sea. Interactions equivalent to the boson gluon graph appear at NLO. This method is used in the H1 2000 pdf fit [12]. The ZEUS-S and ZEUS-JET fits use an interpolation between these approaches, a “variable flavour number scheme” [14].

At HERA energies there are substantial charm and beauty contributions to the proton structure functions. The charm contribution to F_2 is typically 20% to 30%, the beauty contribution was measured to be in the range 0.3% to 3% (see [15]). These numbers suggest to make direct use of the experimental information on charm and beauty production in the pQCD pdf analyses.

8 Conclusion

The structure function F_L provides an important constraint on $g(x)$ and a consistency check for QCD analyses. No direct measurements exist yet at HERA energies.

A new approach based on the observation of jets provides new inclusive DIS data at

high x .

The CC data of HERA allow for a separate determination of u and d pdfs, free of nuclear corrections.

Data on di-jet production can improve pdf-fits at medium x .

The new available data on charm and beauty production may provide direct input for the heavy flavour treatment in pQCD analyses.

HERA II will strongly improve the precision of high Q^2 data.

Acknowledgements

I am grateful to Emmanuelle Perez and Alex Tapper for carefully reading the draft.

References

- [1] see e.g. the talks of M. Bell, N. Berger, D. Dobur, V. Dodonov M. Sutton, these proceedings.
- [2] Yongdok Ri, these proceedings; [H1 Collaboration], arXiv:hep-ex/0512060; [ZEUS Collaboration], arXiv:hep-ex/0602026.
- [3] A. Aktas *et al.* [H1 Collaboration], Phys. Lett. B **632** (2006) 35.
- [4] H1 Collaboration, H1prelim-03-043, contributed paper ICHEP 2004, Beijing.
- [5] C. Adloff *et al.* [H1 Collaboration], Eur. Phys. J. C **21** (2001) 33.
- [6] S. Chekanov *et al.* [ZEUS Collaboration], Phys. Rev. D **67** (2003) 012007.
- [7] A. D. Martin, R. G. Roberts, W. J. Stirling and R. S. Thorne, Eur. Phys. J. C **23** (2002) 73.
- [8] S. Alekhin, Phys. Rev. D **68** (2003) 014002.
- [9] ZEUS Collaboration, contributed paper, Lepton-Photon 2005, Uppsala.
- [10] W. Furmanski and R. Petronzio, Phys. Lett. B **97** (1980) 437.
- [11] S. Chekanov *et al.* [ZEUS Collaboration], Eur. Phys. J. C **42** (2005) 1.
- [12] C. Adloff *et al.* [H1 Collaboration], Eur. Phys. J. C **30** (2003) 1.

- [13] J. Pumplin, D. R. Stump, J. Huston, H. L. Lai, P. Nadolsky and W. K. Tung, JHEP **0207** (2002) 012.
- [14] R. S. Thorne and R. G. Roberts, Phys. Rev. D **57** (1998) 6871.
- [15] M. Bell, these proceedings; A. Aktas *et al.* [H1 Collaboration], Eur. Phys. J. C **45** (2006) 23; Eur. Phys. J. C **40** (2005) 349.